Synthetic and Systems Biotechnology 7 (2022) 1133–1141

Contents lists available at ScienceDirect

Synthetic and Systems Biotechnology

journal homepage: www.keaipublishing.com/en/journals/synthetic-and-systems-biotechnology

Original Research Article

Integrated pathway engineering and transcriptome analysis for improved astaxanthin biosynthesis in *Yarrowia lipolytica*

Dan-Ni Wang [a], Jie Feng [a], Chen-Xi Yu [a], Xin-Kai Zhang [a], Jun Chen [a], Liu-Jing Wei [a], Zhijie Liu [b], Liming Ouyang [a], Lixin Zhang [a], Qiang Hua [a,c], Feng Liu [a,*]

[a] State Key Laboratory of Bioreactor Engineering, East China University of Science and Technology, 130 Meilong Road, Shanghai, 200237, PR China
[b] Key Laboratory of Fermentation Engineering (Ministry of Education), Cooperative Innovation Center of Industrial Fermentation (Ministry of Education & Hubei Province), Hubei Key Laboratory of Industrial Microbiology, Hubei University of Technology, Wuhan, 430068, China
[c] Shanghai Collaborative Innovation Center for Biomanufacturing Technology, 130 Meilong Road, Shanghai, 200237, China

ARTICLE INFO

Keywords:
Astaxanthin
Pathway engineering
Transcriptome analysis
Yarrowia lipolytica

ABSTRACT

Astaxanthin is a high value carotenoid with a broad range of commercial applications due to its superior antioxidant properties. In this study, β-carotene-producing *Yarrowia lipolytica* XK17 constructed in the lab was employed for astaxanthin biosynthesis. The catalytic effects of β-carotene ketolase CrtW and β-carotene hydroxylase CrtZ from various species were investigated. The PspCrtW from *Paracoccus* sp. and HpCrtZ$^{\#}$ from *Haematococcus pluvialis* were confirmed to be the best combination in converting β-carotene. Several key bottlenecks in biomass and astaxanthin biosynthesis were effectively eliminated by optimizing the expression of the above enzymes and restoring uracil/leucine biosynthesis. In addition, the effects of astaxanthin biosynthesis on cell metabolism were investigated by integrated analysis of pathway modification and transcriptome information. After further optimization, strain DN30 was able to synthesize up to 730.3 mg/L astaxanthin in laboratory 5-L fermenter. This study provides a good metabolic strategy and a sustainable development platform for high-value carotenoid production.

1. Introduction

Astaxanthin is a red-orange colored pigment, which widely exists in algae, bacteria and fungi. As a strong antioxidant, astaxanthin possesses tremendous commercial value in feed, nutraceutical and cosmetic industries [1–3]. In current commercial market, the vast majority of astaxanthin is produced via chemical synthesis, but synthetic astaxanthin is not approved for use in human consumption due to the biosafety concern [4,5]. On the other hand, natural astaxanthin is more active and safer than synthetic one, but traditional extraction methods of natural astaxanthin are high-cost and difficult to scale up. Therefore, using microorganisms as efficient platforms for astaxanthin production has attracted considerable attentions [4–6]. In relevant studies, astaxanthin titers in engineered *Escherichia coli*, *Saccharomyces cerevisiae*, and *Y. lipolytica* strains varied from 404.78 mg/L to 3.3 g/L in different culture scales [7–9].

Although lots of efforts have been made for astaxanthin production in engineered microbes, a higher astaxanthin titer is urgently required for cost-effective commercialization, which is mainly due to the poor conversion efficiency of the precursor β-carotene to astaxanthin. Therefore, many strategies have been developed to improve the conversion efficiency of β-carotene to astaxanthin [9–13]. One of the most significant strategies was focused on optimizing the catalytic efficiency of β-carotene ketolase (CrtW) and β-carotene hydroxylase (CrtZ). Tramontin et al. (2019) introduced CrtW and CrtZ derived from *Paracoccus* sp., *Pantoea ananatis* and *Haematococcus pluvialis* into *Y. lipolytica* with different copy numbers, and effectively doubled astaxanthin production [11]. By random mutation of gene *CrtW*, Di et al. (2020) increased the astaxanthin titer in *E. coli* by 5.35-fold. Besides, reducing the steric hindrance between the enzyme and the substrate to accelerate the catalytic reaction is also an effective strategy to improve the conversion efficiency. Ma et al. (2021) targeted the fusion of CrtW (*Paracoccus* sp.) and CrtZ (*H. pluvialis*) to the liposomes, endoplasmic reticulum and peroxisomes in *Y. lipolytica*, the engineered strains eventually produced 139 mg/L astaxanthin in shake flask, which represents a 14-fold increase over the astaxanthin titer of the initial strain [14].

Peer review under responsibility of KeAi Communications Co., Ltd.
* Corresponding author.
E-mail address: fengliu@ecust.edu.cn (F. Liu).

https://doi.org/10.1016/j.synbio.2022.08.001
Received 21 April 2022; Received in revised form 14 July 2022; Accepted 5 August 2022
Available online 18 August 2022

Y. lipolytica as one of the most widely used unconventional yeasts is considered to be a generally recognized as safe (GRAS) microorganism. A series of studies have confirmed the great potential of *Y. lipolytica* as a host for terpenoid production, as it not only possesses sufficient acetyl-CoA supply for terpenoid biosynthesis and large amounts of lipid accumulation for the storage of highly hydrophobic compounds, but also is suitable for large-scale cultivation [15–17]. In addition, several genetic manipulation tools of *Y. lipolytica* have been developed for comprehensive metabolic engineering [18–21]. Especially, to address the limitation of selective markers, a CRISPR/Cas9 system was developed for marker-free gene disruption and integration. A non-homologous end-joining (NHEJ) integration method was also developed for rapid optimization of biosynthetic pathways [22], which further relieved the limitation of the low efficiency of homologous recombination in *Y. lipolytica* [23].

In this study, we successfully constructed several *Y. lipolytica* strains capable of efficiently synthesizing astaxanthin using the in-house β-carotene-producing strain as the initial strain. The design and engineering of the above strains benefited from enzyme source screening and copy number optimization of genes encoding β-carotene ketolase and β-carotene hydroxylase, transcriptome analysis of multiple engineered strains, and laboratory DO-stat fed-batch fermentation. The results of this study provide a better understanding of the engineered strain and further improving its astaxanthin yield.

2. Materials and methods

2.1. Media and culture conditions

E. coli strains were cultured in Luria-Bertani (LB) medium (1% tryptone, 0.5% yeast extract, and 1% NaCl) at 37 °C with shaking (220 rpm). Ampicillin (100 μg/mL) or kanamycin (50 μg/mL) was used for plasmid selection. For *Y. lipolytica* strains, YPD medium (2% peptone, 1% yeast extract, and 2% glucose) was used for cell growth, and YNB medium (0.67% yeast nitrogen base without amino acids, 2% glucose, and 1.5% agar) was used for transformants selection. All *Y. lipolytica* strains were cultured at 30 °C with shaking (220 rpm).

2.2. Construction of plasmids and strains

E. coli DH10B was used for cloning and plasmid construction. The strain XK17 of *Y. lipolytica* was employed as the initial strain, which is deficient in both leucine and uracil biosynthesis [24]. All the strains constructed in this study are listed in Supplementary Table S1. All the plasmids used are shown in Supplementary Table S2, and the primers for plasmid construction are listed in Supplementary Table S3. All astaxanthin biosynthetic genes were codon-optimized towards *Y. lipolytica* and synthesized by Generay Biotechnology (Shanghai, China). PCR amplification was performed using super-fidelity DNA polymerase (Vazyme Biotech Co., Ltd, Nanjing, China). PCR fragments were assembled by using One Step Cloning Kit (Vazyme). Plasmids or linearized plasmids were transformed into *Y. lipolytica* cells by using Yeast Transformation Kit (Zymo Research, Irvine, CA).

In order to screen different genes and optimize gene expression ratio, the CRISPR/Cas9 system of *Y. lipolytica* was utilized [25,26], and several genomic sites have been selected for this strategy in our previous study [24]. To screen strains for higher astaxanthin production, plasmids were linearized and then integrated into the genome via NHEJ-mediated method. The restriction enzymes were purchased from Thermo Fisher Scientific (Waltham, MA). All genes mentioned in this study were placed under the control of the UAS1B8-TEF (136) promoter.

2.3. Extraction and quantification of carotenoids

About 50 μL aliquot of the fermentation broth were taken and centrifuged to collect cell pellets. The cell pellets were suspended in 500 μL dimethyl sulfoxide (DMSO) prior to heating at 55 °C for 30 min, then 500 μL acetone were added and the mixture was heated at 55 °C for 15 min. After filtering through a 0.22 μm pore-size nylon membrane, the supernatants containing carotenoids were analyzed using the Shimadzu LC-20A high performance liquid chromatography (HPLC) instrument (Shimadzu Co., Kyoto, Japan) equipped with a variable-wavelength detector (450 nm) and a ZORBAX SB-Aq column (Agilent Technologies Inc., Santa Clara, CA). The mobile phase (at 40 °C) was acetonitrile/methanol/isopropanol/water (9:6:4:1, v/v) at speed of 1 mL/min. Standard curves of carotenoids (Sigma-Aldrich, St. Louis, MO) were generated by conducting the same extraction method.

2.4. Quantification of byproducts and dry cell weight (DCW)

Byproducts in cell supernatants were determined using an UPLC (Acquity UPLC H-Class, Waters) equipped with a triple quadrupole mass spectrometer (Xevo TQ-XS, Waters). Elution was performed using solvent A (water containing 0.1% formic acid) and solvent B (acetonitrile containing 0.1% formic acid) as the mobile phase at a flow rate of 0.4 mL/min and a temperature of 45 °C. The gradient program was set from 1% to 100% of solvent B. The parameter settings conducted in triple quadrupole MS were shown below: scan speed: 0.01 s/scan, multiple reaction monitoring (MRM) mode, capillary voltage: 1 kV (positive/negative mode), source temperature: 150 °C, desolvation gas temperature: 450 °C, desolvation gas (>99.5% Nitrogen) flow: 900 L/h, cone gas (>99.5% Nitrogen): 50 L/h. Data were acquired by software Masslynx 4.2.

To determine the dry cell weight, 2 mL aliquot of the fermentation broth were taken and centrifuged to collect cells. The cell pellets were washed with milli-Q water for three times, dried at 105 °C for 24 h and weighed after that.

2.5. Analysis of transcriptome

Total RNA extraction and transcriptome sequencing were conducted by Novogene Co. Ltd (Beijing, China). Briefly, RNA integrity was assessed using the RNA Nano 6000 Assay Kit of the Bioanalyzer 2100 system (Agilent). After using total RNA as input material for the RNA sample preparations, library quality was assessed on the Agilent Bioanalyzer 2100 system (Agilent). The clustering of the index-coded samples was performed on a cBot Cluster Generation System using TruSeq PE Cluster Kit v3-cBot-HS (Illumina Inc., San Diego, CA) according to the manufacturer's instructions. After cluster generation, the library preparations were sequenced on an Illumina Novaseq platform and 150 bp paired-end reads were generated. Raw data (raw reads) of fastq format were firstly processed through in-house perl scripts. In this step, clean data (clean reads) were obtained by removing reads containing adapter, reads 1 containing N base and low-quality reads from raw data. At the same time, Q20, Q30 and GC content of the clean data were calculated. Transcriptome data analyzed in this study was provided in Supplementary Table S5. Data analysis was performed on the online platform of the Novomagic Platform (https://magic.novogene.com/customer/main#/login).

2.6. Shake flask culture and fermentation

The engineered strains were firstly plated onto solid YPD medium, then single colony of strains was picked from plate and cultured in 2 mL YPD medium at 30 °C and 220 rpm. The seed culture was inoculated into 250 mL shake flasks containing 50 mL YPD medium (initial OD_{600} = 0.01) and cultivated at 30 °C and 220 rpm for 4 days.

The fed-batch fermentation was carried out at 30 °C in a 5-L fermenter (Baoxing Co., Ltd., Shanghai, China) containing 2 L of 2 × YPD medium (4% peptone, 2% yeast extract, and 4% glucose). Cells were grown in 50 mL YPD medium in a 250 mL flask at 30 °C with shaking (220 rpm) until OD_{600} value reached to between 8 and 10, then

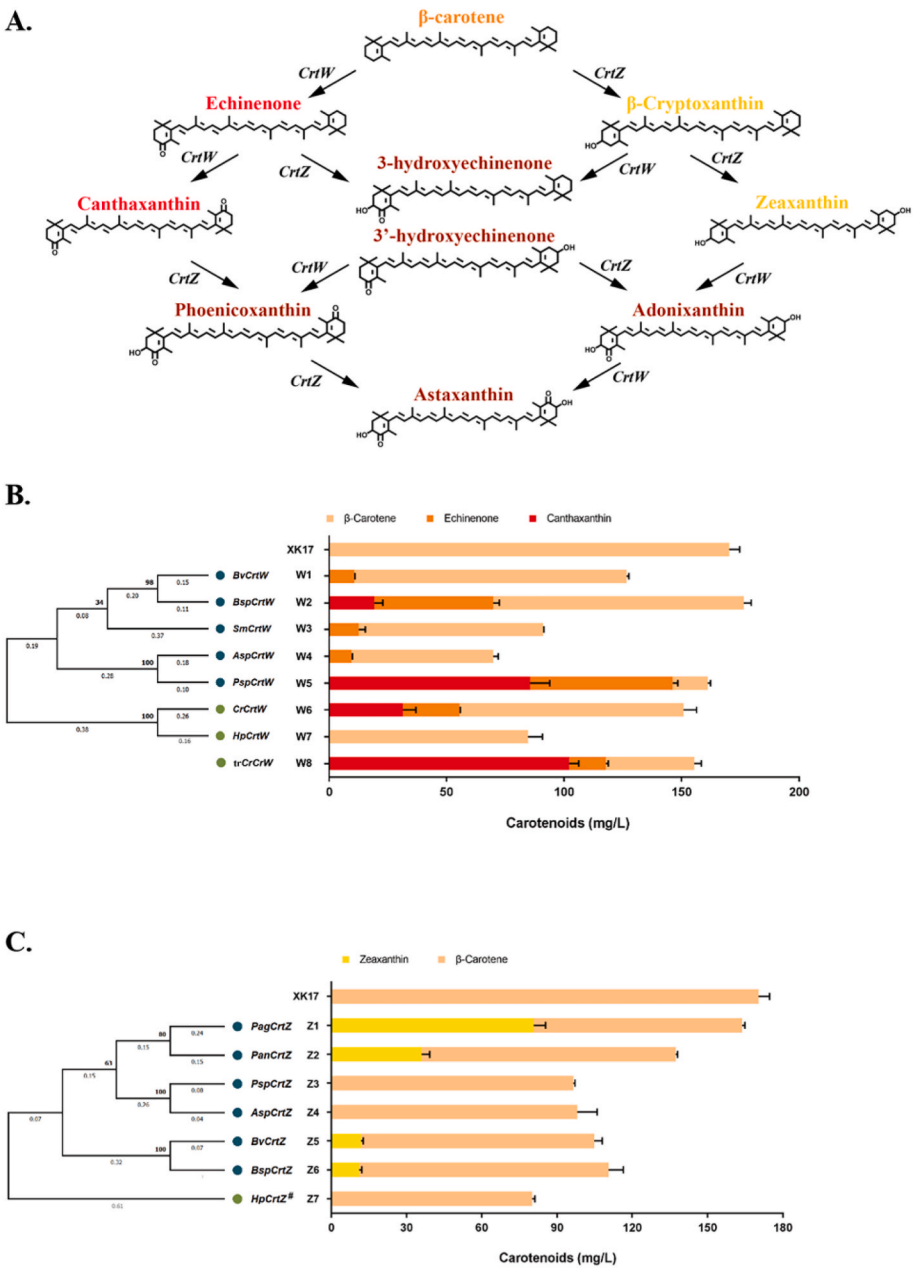

Fig. 1. Screening β-carotene ketolase (CrtW) and hydroxylase (CrtZ) from diverse organisms. (A) The biosynthetic pathway from β-carotene to astaxanthin. (B) Comparing the efficiency of different CrtWs in converting β-carotene to echinenone and canthaxanthin. (C) Comparing the efficiency of different CrtZs in converting β-carotene to β-cryptoxanthin and zeaxanthin (β-cryptoxanthin not detected). Evolutionary trees are constructed by maximum likelihood method, the percentage of trees in which the associated taxa clustered together is shown above the branches. Blue circle, bacteria. Green circle, algae. Error bar represents standard deviation of triplicate experiments.

50 mL of seed culture were inoculated into the fermenter containing the medium saturated by filtered air. The air flux and the agitation rate were set at 2 vvm and 900 rpm. The pH was maintained at 5.5 by feeding 5 M NaOH or 5 M HCl. During fermentation process, the antifoam solution was added to eliminate excessive foam. After complete consumption of glucose (20 h), 80% glucose was pumped into the fermenter to maintain dissolved oxygen (DO) concentration at 25–35%.

3. Results and discussion

3.1. Determination of the catalytic efficiency of CrtW and CrtZ derived from diverse species

In our previous study, the strain *Y. lipolytica* XK17 has been successfully constructed, which was capable to synthesize a significant amount of β-carotene, the key precursor for astaxanthin production [24]. Although only two enzymes (CrtW and CrtZ) are required to convert β-carotene to astaxanthin, the conversion process occurs in six different ways, resulting in up to eight metabolic intermediates (Fig. 1A). It has been reported that CrtW and CrtZ showed diverse substrate affinity and enzymatic activity in different host microorganisms [27–31], suggesting that the conversion pathways of β-carotene to astaxanthin and the proportion of astaxanthin in total carotenoids are greatly affected by different sources of CrtW and CrtZ. Therefore, in order to obtain the appropriate CrtW/CrtZ combination for astaxanthin synthesis in *Y. lipolytica*, we selected 7 CrtZs and 8 CrtWs from 9 bacteria and microalgae for CrtW/CrtZ combination expression experiments (Fig. 1B and C).

We first selected β-carotene ketolase from multiple sources and evaluated their ability to convert β-carotene into echinenone and canthaxanthin in *Y. lipolytica*. The tested CrtWs were taken from *Brevundimonas vesicularis* DC263 (BvCrtW), *Brevundimonas* sp. SD212 (BspCrtW), *Sphingomonas melonis* DC18 (SmCrtW), *Alcaligenes* sp. PC-1 (AspCrtW), *Paracoccus* sp. N81106 (PspCrtW), *Chlamydomonas reinhardtii* (CrCrtW) and *H. pluvialis* (HpCrtW), respectively, as well as a truncated CrCrtW (trCrCrtW) because of its reported higher catalytic

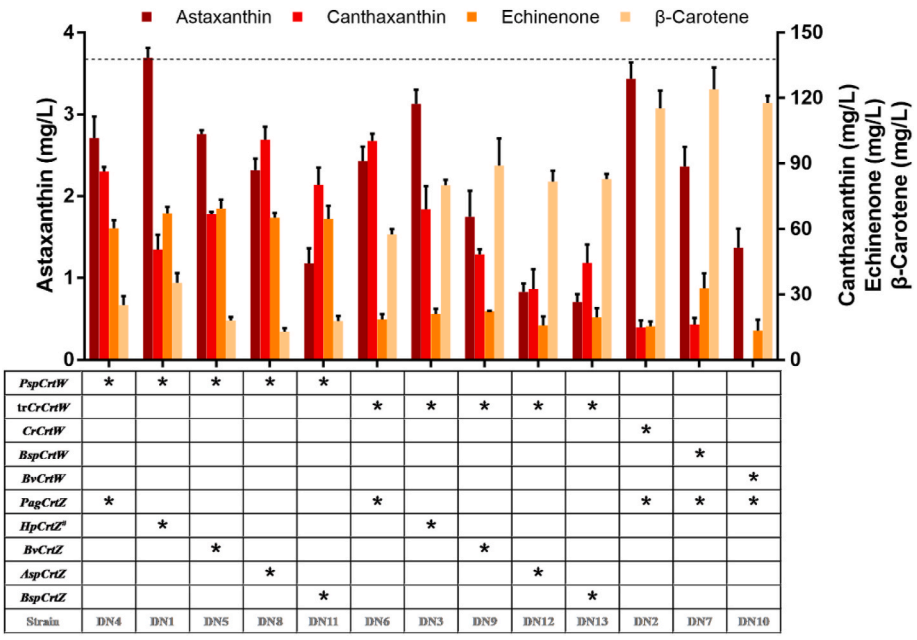

Fig. 2. Combinatorial optimization of CrtW and CrtZ from diverse organisms. Carotenoids titers were determined in 13 strains expressing CrtW and CrtZ from various sources (other hydroxycarotenoids not detected). The different CrtW/CrtZ combinations are marked with asterisks under each group of bars. Error bar represents standard deviation of triplicate experiments.

activity in astaxanthin synthesis [32,33]. Each *CrtW* gene was codon-optimized and individually integrated into the genome of strain XK17 (A1 locus) by using CRISPR/Cas9 strategy to obtain the constructed strains W1 to W8. As shown in Fig. 1B, all CrtWs except HpCrtW could catalyze the conversion of β-carotene into echinenone or canthaxanthin, where PspCrtW and trCrCrtW showed higher conversion efficiency compared with other CrtWs. In addition, PspCrtW could convert most β-carotene to echinenone and canthaxanthin, while trCrCrtW showed a better conversion performance of echinenone to canthaxanthin. Consistent with the literature results, we also found that the truncated CrCrtW had a higher β-carotene conversion efficiency compared to CrCrtW, and it is therefore necessary to further evaluate its effect on the synthesis of astaxanthin.

Next, we focused on seven CrtZs to evaluate their ability of converting β-carotene into zeaxanthin, in which PagCrtZ from *Pantoea agglomerans*, PanCrtZ from *P. ananatis*, PspCrtZ from *Paracoccus* sp. N81106, AspCrtZ from *Alcaligenes* sp. PC-1, BvCrtZ from *B. vesicularis* DC263, BspCrtZ from *Brevundimonas* sp. SD212, and HpCrtZ$^{\#}$ from a variant CrtZ of *H. pluvialis* with a site mutation K82R (HpCrtZ$^{\#}$ has been proven to be stable without being ubiquitinated) [34,35]. The efficiency of each β-carotene hydroxylase to convert β-carotene to zeaxanthin was evaluated (no accumulation of β-cryptoxanthin was detected in any of these cases). Each *CrtZ* gene was codon-optimized and individually integrated into the genome of strain XK17 (E1 locus) by using CRISPR/Cas9 strategy, resulting in strains Z1 to Z7 (Fig. 1C). Surprisingly, only four CrtZs showed limited hydroxylation of β-carotene. Even PagCrtZ with the best catalytic effect could only convert approximately 48% of β-carotene into zeaxanthin.

In order to further evaluate the co-expression effects of CrtW and CrtZ on astaxanthin biosynthesis from β-carotene, we introduced the

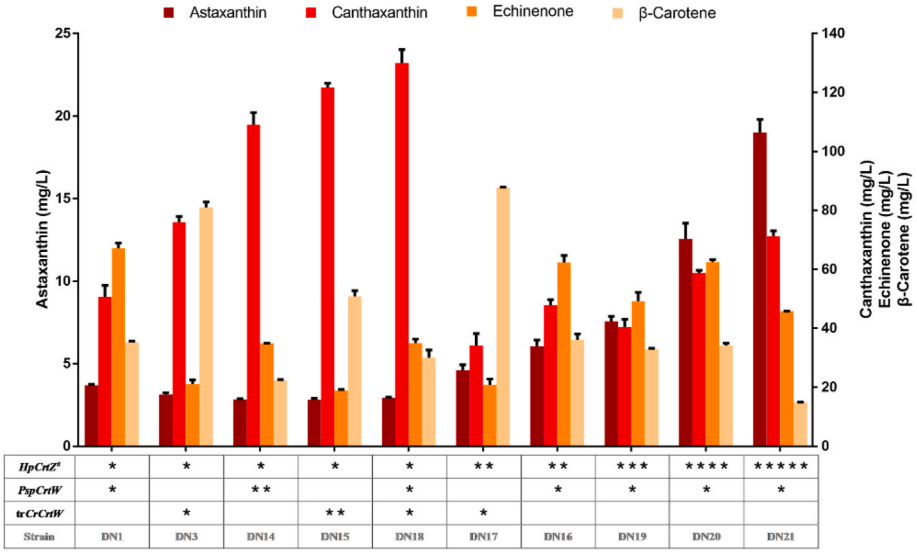

Fig. 3. Effects of copy number of the *PspCrtW*, *trCrCrtW* and *HpCrtZ*$^{\#}$ genes on carotenoids biosynthesis (hydroxycarotenoid not detected). The copy number of the corresponding gene is indicated by the number of asterisks. Error bar represents standard deviation of triplicate experiments.

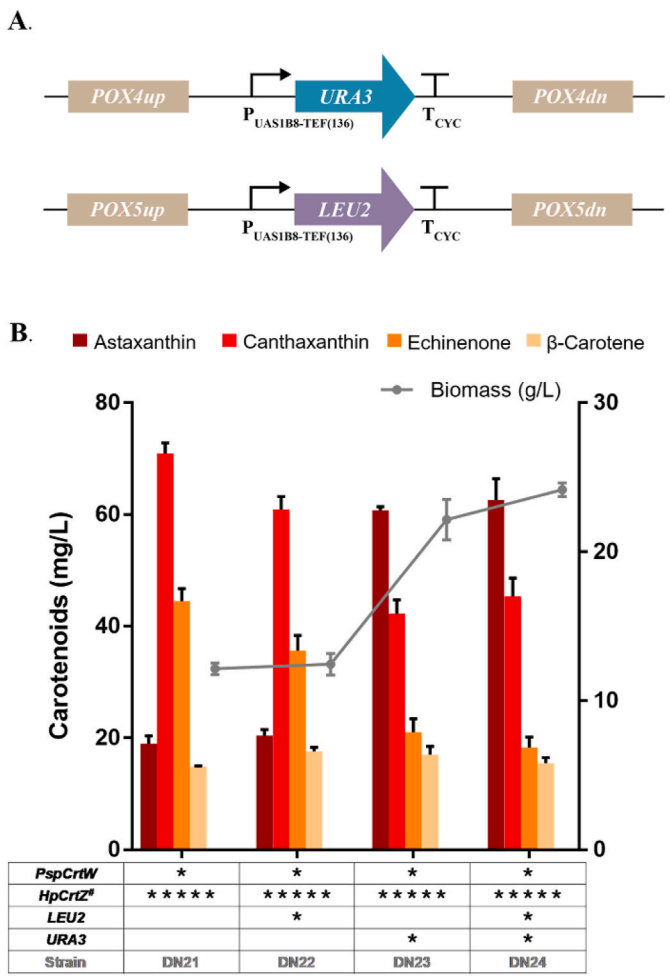

Fig. 4. Restoring uracil or/and leucine biosynthesis in strain DN21. (A) Two linear DNA fragments harboring the URA3 marker and the LEU2 marker, respectively. Bent arrow: a promoter; T-shape bar: a transcription terminator. (B) Biomass and carotenoids production of strains restoring uracil or/and leucine biosynthesis. The copy number of the corresponding genes is indicated by the number of asterisks. Error bar represents standard deviation of triplicate experiments.

above 7 *CrtZ* genes into strains W5 and W8, respectively, using the same CRISPR/Cas9 integration method and resulting in 14 engineered strains with different CrtW/CrtZ combinations. Similarly, except *PspCrtW* and *trCrCrtW* genes, the other six *CrtW* genes were expressed respectively into strain Z1 which showed better hydroxylation of β-carotene. Interestingly, astaxanthin synthesis was detected in only 13 of the 20 engineered strains (Fig. 2). We observed that the amount of astaxanthin synthesized and the amount of β-carotene remaining in the above strains were significantly affected by the combination of CrtW and CrtZ. In accordance with the strain W5 in Fig. 1B, the introduction of PspCrtW always resulted in efficient ketolation of β-carotene and intracellular β-carotene content below 40 mg/L. Although the strain co-expressed by PagCrtZ and PspCrtW (DN4) and the strain co-expressed by PagCrtZ and trCrCrtW (DN6) showed high astaxanthin biosynthesis, replacing PagCrtZ with HpCrtZ$^{\#}$ increased astaxanthin production by approximately 30% (strains DN1 and DN3, respectively). Considering the fact that HpCrtZ$^{\#}$ could not hydroxylate β-carotene into zeaxanthin (Fig. 1C), we inferred that HpCrtZ$^{\#}$ might have higher catalytic specificity and activity only for ketocarotenoids. Another interesting observation was that astaxanthin production of strain DN2 (CrCrtW/PagCrtZ) was about 50% higher than that of strain DN6 (trCrCrtW/PagCrtZ). Since Fig. 1B shows that more canthaxanthin was ketolated from β-carotene by trCrCrtW than by CrCrtW, we may conclude that CrCrtW can catalyze the ketolation of hydroxylated carotenoids more efficient than trCrCrtW, a product of 117 amino acids truncated from the C-terminus of CrCrtW.

3.2. Optimization of CrtW/CrtZ expression ratio

Strain DN1 harboring PspCrtW/HpCrtZ$^{\#}$ and strain DN3 harboring trCrCrtW/HpCrtZ$^{\#}$ both showed good astaxanthin synthesis and were selected to investigate the effect of copy number of these genes in these two strains. By comparing DN14 with DN1, and DN15 with DN3, we found that the introduction of one additional *PspCrtW* gene or *trCrCrtW* gene promoted more canthaxanthin synthesis, but had no effect on astaxanthin synthesis. So did the strain DN18, in which one PspCrtW and one trCrCrtW were introduced together with an HpCrtZ$^{\#}$ (Fig. 3). These results suggested that hydroxylation of ketocarotenoids is critical for astaxanthin biosynthesis in these engineered strains. This was well demonstrated by the introduction of another HpCrtZ$^{\#}$ in either strain DN1 or DN3, which resulted in a 40%–50% increase in astaxanthin biosynthesis with a significant reduction in canthaxanthin content (strains DN16 and DN17 in Fig. 3). Encouraged by this, we further increased the copy number of HpCrtZ$^{\#}$ in strain DN16 to 5 copies (strains DN19 to DN21). Each additional copy number of HpCrtZ$^{\#}$ resulted in a 1.3 – 1.5-fold increase in astaxanthin production. The strain DN21 with one PspCrtW and five HpCrtZ$^{\#}$ could produce approximately 19 mg/L astaxanthin, 5-fold higher than that in strain DN1. Accordingly, the proportion of astaxanthin in carotenoids increased significantly from 2% in strain DN1 to 12% in strain DN21.

3.3. Effect of auxotrophy on cell growth and astaxanthin production

Since the above studies were based on the uracil and leucine auxotrophic strain, the restoring of nutritional requirements may greatly affect cell growth and the biosynthesis of target product. Linear DNA fragment containing *LEU2* or *URA3* was constructed and transformed into strain DN21 to obtain strains DN22 and DN23, respectively (Fig. 4A). The results showed that restoring uracil biosynthesis doubled the cell growth and tripled the astaxanthin titer (approximately 2.5 mg astaxanthin/g DCW, DN23), while restoring leucine biosynthesis was not effective in promoting cell growth and astaxanthin synthesis (strains DN22 and DN24, Fig. 4B). These findings were not consistent with the report of Schwartz et al. (2017) that *Y. lipolytica* growth and lycopene biosynthesis were increased only when both nutritional requirements were complemented [36]. Interestingly, the total carotenoids produced by strains DN22 to DN24 did not change much compared with that of strain DN21 (Fig. 4B), so astaxanthin synthesized by strains with restored uracil or uracil/leucine synthesis rapidly increased to about 50% of the total carotenoids.

3.4. Transcriptome analysis of different carotenoid-producing strains

The biosynthesis of astaxanthin has been improved by screening and optimizing copy numbers of the *CrtW* and *CrtZ* genes, and restoring uracil biosynthesis. Next, we conducted transcriptome analysis to study how the introduction of astaxanthin biosynthesis steps affects cell metabolism and regulation, so as to provide useful information for better promoting astaxanthin biosynthesis and improving the proportion of astaxanthin in total carotenoids. Therefore, the uracil requirements of β-carotene-producing strain XK17, astaxanthin-producing strains DN1 and DN21 with different copy numbers of astaxanthin biosynthesis genes were complemented to obtain strains DN25, DN26, and DN23 (Fig. 5A). The results showed that the total carotenoid production of strains DN23 and DN26 was about 60% lower than that of strain DN25, indicating that the excess introduction of the astaxanthin biosynthesis pathway affected the carbon flux toward the carotenoid biosynthesis. By analyzing the time course of β-carotene/astaxanthin production in

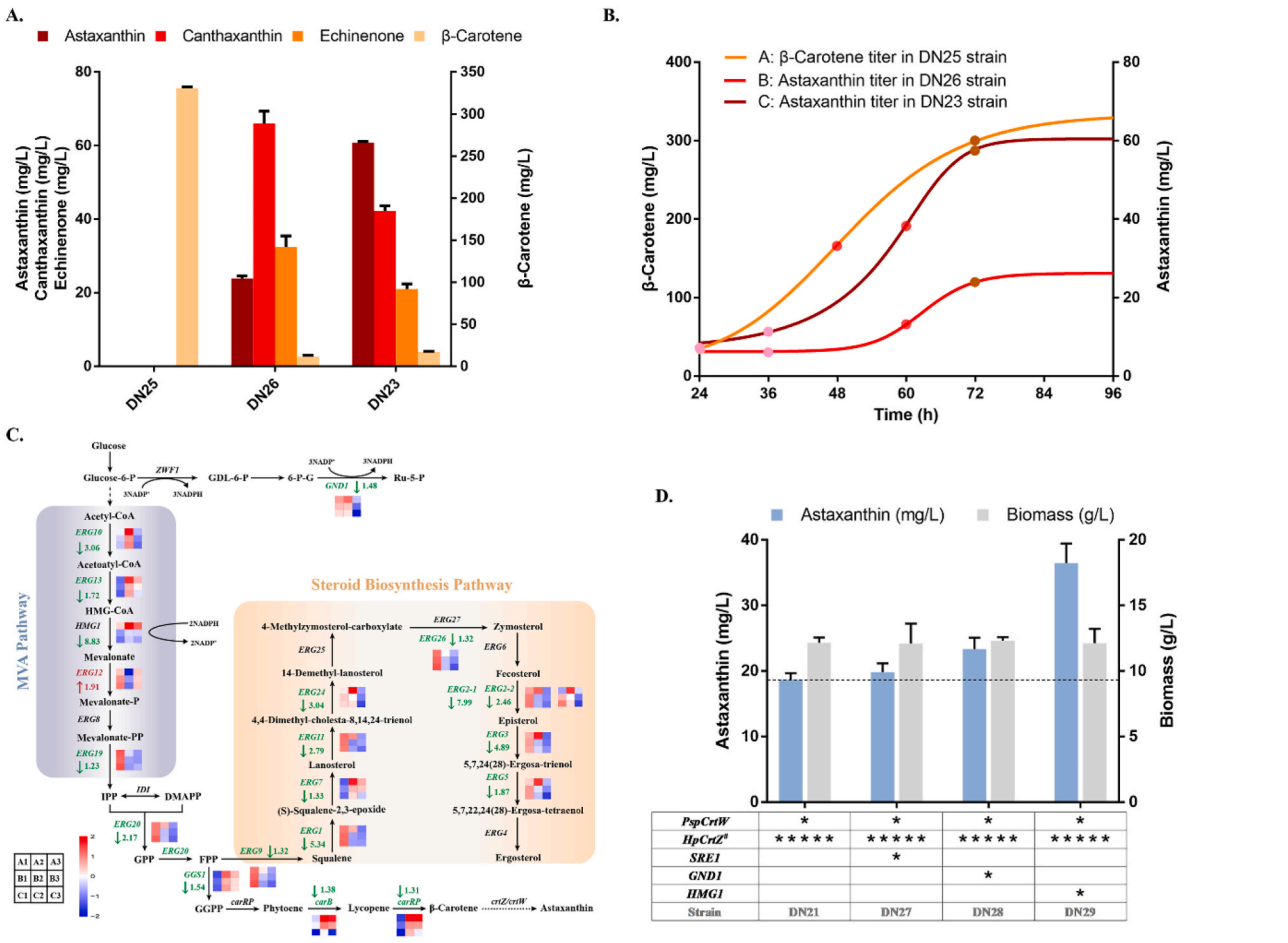

Fig. 5. Transcriptome analysis of different carotenoid-producing strains. (A) Carotenoid production of strains DN25, DN26 and DN23. (B) β-carotene/astaxanthin production curves of strain DN25, strains DN23 and DN26. For each strain, we selected three samples (A, B, C) with different β-carotene/astaxanthin productivity for transcriptome analysis. Pink circle: early stage; Red circle: middle stage; Brown circle: final stage. (C) Expression pattern of genes involved in the MVA pathway and steroid biosynthesis pathway. Green or red arrows represent the down-regulation or up-regulation of gene transcriptions in Group B2 relative to Group A2. Values represent the corresponding fold changes. (D) Carotenoids production and biomass of strains overexpressing key genes based on transcriptome analysis.

above three strains, two points with the highest and lowest productivity of astaxanthin and a transition point between them were determined and set as the first, second and third stage respectively (Fig. 5B, Supplementary Fig. S2 and Table S4). Subsequently, transcriptome analysis was performed on the obtained strains DN25, DN26, and DN23 at these three stages (Supplementary Fig. S1). Principal component analysis (PCA) showed that the gene transcription patterns of the above three strains were basically the same at the first and third stages. The transcription of strain DN25 (A) was, however, significantly different from strain DN26 (B) and strain DN23(C) at the second stage. Therefore, the following analysis only focused on the corresponding transcriptomic data.

RNA-sequencing (RNA-seq) data analysis of strains DN25 and DN26 in the second production stage (B2 vs A2) showed that a total of 1584 differentially expressed genes (DEGs) ($p < 0.05$; $|\log_2 FC| \geq 1$), including 631 up-regulated genes and 953 down-regulated genes in strain DN26 when compared to strain DN25 (Supplementary Fig. S1B). As expected, KEGG pathway enrichment analysis indicated that compared to the genes in strain DN25, transcription levels of most genes involved in the mevalonate (MVA) pathway and ergosterol biosynthetic pathway were significantly down-regulated in strain DN26. Especially the *HMG1*, *ERG1*, *ERG3* and *ERG2-1* genes were down-regulated 8.8-fold, 5.3-fold, 4.9-fold and 8.0-fold, respectively (Fig. 5C and Supplementary Fig. S1C). The MVA pathway is well-known to provide key precursors for carotenoids biosynthesis in *Y. lipolytica* [37]. Sterol esters synthesized from ergosterol is one of the main components of lipid droplets, which plays a key role in carotenoid accumulation [38–41]. SRE1 is reported as a regulatory element that positively regulates ergosterol biosynthetic pathway genes and the MVA pathway genes in *Xanthophyllomyces dendrorhous* [42–44]. If SRE1 has a similar function in *Y. lipolytica*, the nearly 4-fold down-regulation in its transcription was probably responsible for the significant decrease in transcription levels of genes in the MVA and ergosterol biosynthetic pathways in strain DN26 (Supplementary Table S5). In addition, an adequate supply of NADPH generally facilitates lipid and terpenoid biosynthesis [45–47]. It has been reported that the oxidative pentose phosphate (PP) pathway is the primary source of NADPH in *Y. lipolytica* [48], and we found most DEGs in the PP pathway of strain DN26 were also down-regulated (Supplementary Table S5). Thus, improving the PP pathway flux to increase the supply of cofactor NADPH may also be necessary to promote total carotenoid production and astaxanthin biosynthesis. Both β-carotene and astaxanthin can effectively protect membrane phospholipids and other lipids against the toxicity from reactive oxygen species (ROS) [49]. Therefore, DEGs involved in stress response were also analyzed based on the obtained transcriptome data. Most DEGs in the antioxidant system of strain DN26 were also down-regulated, such as the genes encoding superoxide dismutase SOD1, peroxiredoxin PRDX5 and catalase CTT1 (Supplementary Table S5). Among them, a gene encoding catalase CTT1 (YALI0_E34265g) was 24-fold down-regulated in strain DN26 compared with that in strain DN25. Catalase CTT1 is known to play an important

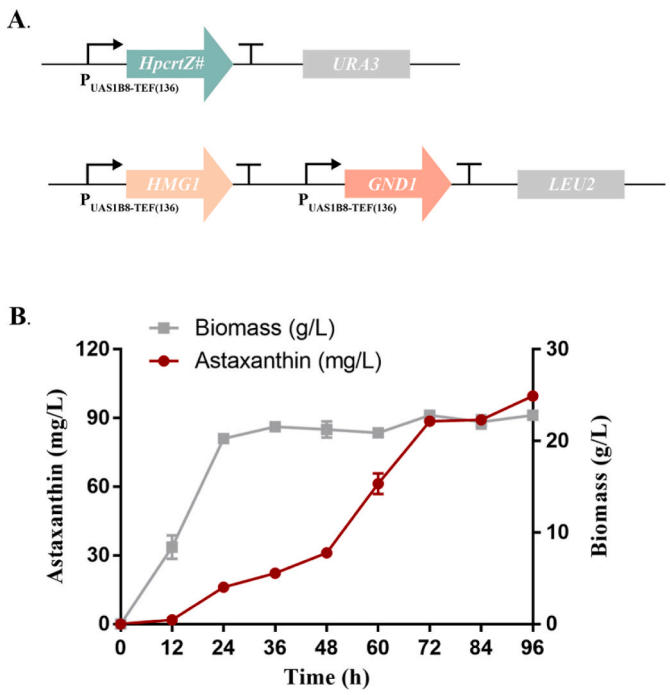

Fig. 6. Construction of strain DN30 by NHEJ-mediated integration. (A) Two linear DNA fragments used to overexpress *HpCrtZ*$^{\#}$, *GND1* and *HMG1* genes into strain DN21 by NHEJ-mediated integration. Bent arrow: a promoter; T-shape bar: a transcription terminator. (B) Astaxanthin production and biomass formation of strain DN30 in shake flasks.

role in the prevention of oxidative damage. Considering that the cell yield of astaxanthin (even total carotenoids) in strain DN26 was much lower than that of β-carotene in strain DN25 (Fig. 5A), the above results strongly suggested that the accumulation of astaxanthin and other carotenoids such as canthaxanthin could more effectively alleviate oxidative stress in *Y. lipolytica*.

Based on the transcriptome analysis, we overexpressed the *SRE1* gene using the CRISPR/Cas9 system in the astaxanthin-producing strain DN21 to increase the amount of carotenoids flux. However, the results indicated that the additional introduction of the *SRE1* gene (strain DN27) did not lead to more accumulation of astaxanthin and total carotenoids, which suggested that the expression of *SRE1* gene is probably regulated by other factors in *Y. lipolytica* (Fig. 5D). Transcriptome analysis also showed that the transcription levels of the *HMG1* gene that encodes a key rate-limiting enzyme of the MVA pathway, and the *GND1* gene that encodes phosphorgluconate dehydrogenase in the oxidative PP pathway to provide reducing equivalent of NADPH, were positively related to astaxanthin production. Further enhancement of these two genes in the strain may also promote the biosynthesis of astaxanthin. The strain DN28 with overexpressed *GND1* gene and the strain DN29 with overexpressed *HMG1* gene were therefore constructed based on the strain DN21. We observed that the additional supply of NADPH increased astaxanthin biosynthesis by about 21%, while the introduction of additional *HMG1* gene led to a rapid increase in astaxanthin production of nearly twice as much (Fig. 5D).

3.5. Synthetic construction of astaxanthin-producing strain by NHEJ-mediated integration and DO-stat fermentation

In addition to the above results, it was observed that the introduction of an additional copy of *HpCrtZ*$^{\#}$ also helped to further pull carotenoid synthesis flow towards astaxanthin biosynthesis (data not shown). As an unconventional yeast, *Y. lipolytica* shows a strong preference for repairing DNA double-strand breaks by NHEJ [23]. In the process of NHEJ-mediated integration, the DNA fragments can be randomly integrated in different chromosomal locations, which may lead to insertional mutagenesis [50]. Therefore, this method is helpful to quickly generate an insertional mutagenesis library to screen out engineered strains with higher yield than expected. In order to synthetically include several genes and necessary nutritional requirements that could effectively promote astaxanthin synthesis into strain DN21, we established a combinatorial library by the NHEJ-mediated method. Two linear DNA fragments, one with codon-optimized gene *HpCrtZ*$^{\#}$ and *URA3*, the other with endogenous genes *HMG1*, *GND1*, and *LEU2*, were constructed and simultaneously transformed into strain DN21 (Fig. 6A). Twenty dark red colonies were picked up by visualization and cultivated in flasks for 4 days (Supplementary Fig. S3). The synthetically engineered strain with the highest astaxanthin production in shake-flask culture was therefore obtained, and the resulting strain DN30 accumulated 99.3 mg/L astaxanthin (about 68% of the total carotenoids), which was approximately 27 times that of strain DN1 and 1.6 times that of strain DN23 (Fig. 6B).

In order to further evaluate the potential of strain DN30 to produce astaxanthin, fed-batch fermentation was performed in 5-L fermenter (Fig. 7A). It has been reported that DO-stat fed-batch fermentation contributes to the improvement of glucose utilization by reducing the Crabtree effect [51], thereby increasing biomass amount. The DO-stat strategy was employed to enhance cell growth and then promote astaxanthin production. YPD20 medium was used as the initial medium. After the initial glucose was exhausted, the rate of feeding (80% glucose) was controlled to maintain a balance between oxygen consumption and supply, automatically meeting the DO set point (30%). Finally, 730.3 mg/L astaxanthin (i.e. 8.9 mg/g DCW) was obtained after 4 days of fermentation (Fig. 7B). However, we also observed that the intermediates echinenone and canthaxanthin kept accumulating during the fermentation, suggesting that although β-carotene hydroxylases have been well screened and improved, their catalytic efficiency needs to be further optimized for large-scale fermentation (Fig. 7C). In addition, the supernatant samples at 96 h of fermentation were measured by LC-MS, and we found that most of organic acids in the TCA cycle were secreted during the fermentation process (Supplementary Fig. S4). It is suggested that it is of great importance to balance the trade-off between the TCA cycle and terpene synthesis for efficiently directing carbon flux towards the astaxanthin biosynthesis.

In previous studies, Ma et al. (2021) constructed a *Y. lipolytica* strain that could produce 453 mg/L of astaxanthin in 5-L fermenter through targeting the enzyme fusions (CrtW-Z) to subcellular compartment [14]. Zhu et al. (2022) adjusted the expression levels of CrtW and CrtZ, restored leucine biosynthesis, and performed fed-batch fermentation in the synthetic CSM-Ura medium supplemented with YAG concentrated medium, resulting in the production of 3.3 g/L astaxanthin [9]. Above studies enhanced the production of astaxanthin by promoting the cell growth and substrate conversion. In this study, we firstly obtained a new pair of CrtW and CrtZ for enhancing the conversion of β-carotene, then analyzed the effect of astaxanthin heterologous biosynthesis pathway on cell metabolism and finally determined the rate-limiting steps, which provides promising strategies for the study of microbial heterologous biosynthesis of astaxanthin.

4. Conclusion

Due to the high cost of astaxanthin extraction from nature, metabolic engineering of microorganisms for astaxanthin production has become an attractive strategy. In this study, based on an in-house β-carotene-producing strain and combined analysis of metabolic pathway and transcriptome, we successfully constructed a *Y. lipolytica* strain capable of efficiently synthesizing astaxanthin. Although only preliminary DO-stat fed-batch fermentations were performed, the engineered strain was still able to produce up to 730 mg/L astaxanthin. The results suggested that astaxanthin could be synthesized more efficiently under the optimized cell growth conditions, and could then be employed to a

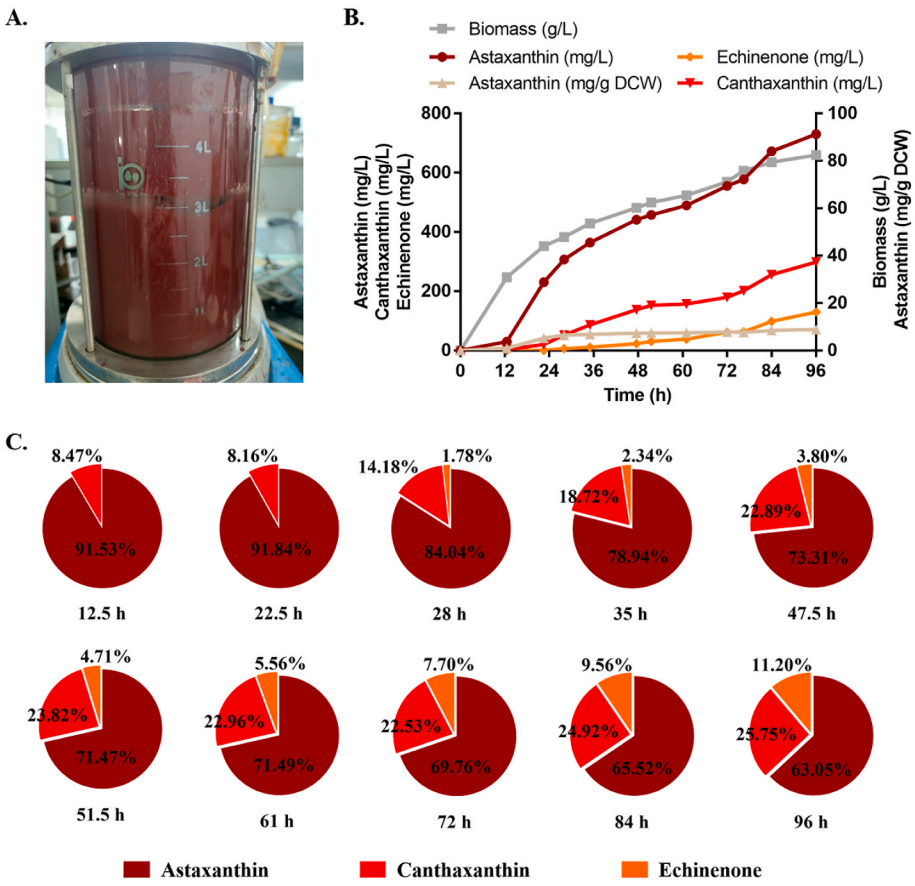

Fig. 7. DO-stat fed-batch fermentation of the engineered strain DN30. (A) Final fermentation broth in 5-L fermenter. (B) DO-stat fed-batch fermentation curves of strain DN30. (C) Changes in the proportion of carotenoids during fermentation. Astaxanthin, canthaxanthin and echinenone were labeled in dark red, red and orange, respectively. Accumulations of β-carotene and other hydroxycarotenoids were not detected.

variety of industrial scenarios. Additionally, little is known about transcription factors regulating terpenoid biosynthesis pathways in *Y. lipolytica*, and further studies are still required. On the other hand, the introduction of novel precursor supply pathway, like the isopentenol utilization pathway, may also contribute to the enhancement of carbon flux towards astaxanthin biosynthesis.

CRediT authorship contribution statement

Dan-Ni Wang: Methodology, Investigation, Data curation, Formal analysis, Writing – original draft. **Jie Feng:** Investigation, Data curation. **Chen-Xi Yu:** Investigation. **Xin-Kai Zhang:** Investigation. **Jun Chen:** Investigation. **Liu-Jing Wei:** Investigation. **Zhijie Liu:** Investigation. **Liming Ouyang:** Conceptualization. **Lixin Zhang:** Conceptualization. **Qiang Hua:** Conceptualization, Funding acquisition, Writing – review & editing. **Feng Liu:** Conceptualization, Funding acquisition, Writing – review & editing.

Declaration of competing interest

The authors declare that they have no known competing financial interests or personal relationships that could have appeared to influence the work reported in this paper.

Acknowledgement

This study was supported by the National Key R&D Program of China (2017YFE0115600, 2019YFA0904302, 2020YFA0907800); and the National Natural Science Foundation of China (21576089, 21776081).

Appendix A. Supplementary data

Supplementary data to this article can be found online at https://doi.org/10.1016/j.synbio.2022.08.001.

References

[1] Ambati RR, Phang SM, Ravi S, Aswathanarayana RG. Astaxanthin: sources, extraction, stability, biological activities and its commercial applications–a review. Mar Drugs 2014;12(1):128–52. https://doi.org/10.3390/md12010128.
[2] Yuan JP, Peng J, Yin K, Wang JH. Potential health-promoting effects of astaxanthin: a high-value carotenoid mostly from microalgae. Mol Nutr Food Res 2011;55(1):150–65. https://doi.org/10.1002/mnfr.201000414.
[3] Jiang GL, Zhou LY, Wang YT, Zhu MJ. Astaxanthin from Jerusalem artichoke: production by fed-batch fermentation using *Phaffia rhodozyma* and application in cosmetics. Process Biochem 2017;63:16–25. https://doi.org/10.1016/j.procbio.2017.08.013.
[4] Wan X, Zhou XR, Moncalian G, Su L, Chen WC, Zhu HZ, et al. Reprogramming microorganisms for the biosynthesis of astaxanthin via metabolic engineering. Prog Lipid Res 2021;81:101083. https://doi.org/10.1016/j.plipres.2020.101083.
[5] Stachowiak B, Szulc P. Astaxanthin for the food industry. Molecules 2021;26(9):2666. https://doi.org/10.3390/molecules26092666.
[6] Lyu X, Lyu Y, Yu H, Chen W, Ye L, Yang R. Biotechnological advances for improving natural pigment production: a state-of-the-art review. Bioresour Bioprocess 2022;9(1):1–38. https://doi.org/10.1186/s40643-022-00497-4.
[7] Gong Z, Wang H, Tang J, Bi C, Li Q, Zhang X. Coordinated expression of astaxanthin biosynthesis genes for improved astaxanthin production in *Escherichia coli*. J Agric Food Chem 2020;68(50):14917–27. https://doi.org/10.1021/acs.jafc.0c05379.
[8] Jiang G, Yang Z, Wang Y, Yao M, Chen Y, Xiao W, et al. Enhanced astaxanthin production in yeast via combined mutagenesis and evolution. Biochem Eng J 2020;156:107519. https://doi.org/10.1016/j.bej.2020.107519.
[9] Zhu HZ, Jiang S, Wu JJ, Zhou XR, Liu PY, Huang FH, et al. Production of high levels of 3S,3'S-astaxanthin in *Yarrowia lipolytica* via iterative metabolic engineering. J Agric Food Chem 2022;70(8):2673–83. https://doi.org/10.1021/acs.jafc.1c08072.

[10] Wang R, Gu X, Yao M, Pan C, Liu H, Xiao W, et al. Engineering of β-carotene hydroxylase and ketolase for astaxanthin overproduction in *Saccharomyces cerevisiae*. Front Chem Sci Eng 2017;11(1):89–99. https://doi.org/10.1007/s11705-017-1628-0.
[11] Tramontin LRR, Kildegaard KR, Sudarsan S, Borodina I. Enhancement of astaxanthin biosynthesis in oleaginous yeast *Yarrowia lipolytica* via microalgal pathway. Microorganisms 2019;7(10):472. https://doi.org/10.3390/microorganisms7100472.
[12] Zhou P, Li M, Shen B, Yao Z, Bian Q, Ye L, et al. Directed coevolution of beta-carotene ketolase and hydroxylase and its application in temperature-regulated biosynthesis of astaxanthin. J Agric Food Chem 2019;67(4):1072–80. https://doi.org/10.1021/acs.jafc.8b05003.
[13] Li D, Li Y, Xu J-Y, Li Q-Y, Tang J-L, Jia S-R, et al. Engineering CrtW and CrtZ for improving biosynthesis of astaxanthin in *Escherichia coli*. Chin J Nat Med 2020;18(9):666–76. https://doi.org/10.1016/s1875-5364(20)60005-x.
[14] Ma Y, Li J, Huang S, Stephanopoulos G. Targeting pathway expression to subcellular organelles improves astaxanthin synthesis in *Yarrowia lipolytica*. Metab Eng 2021;68:152–61. https://doi.org/10.1016/j.ymben.2021.10.004.
[15] Muhammad A, Feng X, Rasool A, Sun W, Li C. Production of plant natural products through engineered *Yarrowia lipolytica*. Biotechnol Adv 2020;43:107555. https://doi.org/10.1016/j.biotechadv.2020.107555.
[16] Li ZJ, Wang YZ, Wang LR, Shi TQ, Sun XM, Huang H. Advanced strategies for the synthesis of terpenoids in *Yarrowia lipolytica*. J Agric Food Chem 2021;69(8):2367–81. https://doi.org/10.1021/acs.jafc.1c00350.
[17] Liu Y, Wang Z, Cui Z, Qi Q, Hou J. α-Farnesene production from lipid by engineered *Yarrowia lipolytica*. Bioresour Bioprocess 2021;8(1):1–12. https://doi.org/10.1186/s40643-021-00431-0.
[18] Shi TQ, Huang H, Kerkhoven EJ, Ji XJ. Advancing metabolic engineering of *Yarrowia lipolytica* using the CRISPR/Cas system. Appl Microbiol Biotechnol 2018;102(22):9541–8. https://doi.org/10.1007/s00253-018-9366-x.
[19] Liu HH, Madzak C, Sun ML, Ren LJ, Song P, Huang H, et al. Engineering *Yarrowia lipolytica* for arachidonic acid production through rapid assembly of metabolic pathway. Biochem Eng J 2017;119:52–8. https://doi.org/10.1016/j.bej.2016.12.004.
[20] Celinska E, Ledesma-Amaro R, Larroude M, Rossignol T, Pauthenier C, Nicaud JM. Golden gate assembly system dedicated to complex pathway manipulation in *Yarrowia lipolytica*. Microb Biotechnol 2017;10(2):450–5. https://doi.org/10.1111/1751-7915.12605.
[21] Bordes F, Fudalej F, Dossat V, Nicaud JM, Marty A. A new recombinant protein expression system for high-throughput screening in the yeast *Yarrowia lipolytica*. J Microbiol Methods 2007;70(3):493–502. https://doi.org/10.1016/j.mimet.2007.06.008.
[22] Cui Z, Jiang X, Zheng H, Qi Q, Hou J. Homology-independent genome integration enables rapid library construction for enzyme expression and pathway optimization in *Yarrowia lipolytica*. Biotechnol Bioeng 2019;116(2):354–63. https://doi.org/10.1002/bit.26863.
[23] Wagner JM, Alper HS. Synthetic biology and molecular genetics in non-conventional yeasts: current tools and future advances. Fungal Genet Biol 2016;89:126–36. https://doi.org/10.1016/j.fgb.2015.12.001.
[24] Zhang XK, Wang DN, Chen J, Liu ZJ, Wei LJ, Hua Q. Metabolic engineering of beta-carotene biosynthesis in *Yarrowia lipolytica*. Biotechnol Lett 2020;42(6):945–56. https://doi.org/10.1007/s10529-020-02844-x.
[25] Schwartz CM, Hussain MS, Blenner M, Wheeldon I. Synthetic RNA polymerase III promoters facilitate high-efficiency CRISPR-Cas9-mediated genome editing in *Yarrowia lipolytica*. ACS Synth Biol 2016;5(4):356–9. https://doi.org/10.1021/acssynbio.5b00162.
[26] Schwartz C, Shabbir-Hussain M, Frogue K, Blenner M, Wheeldon I. Standardized markerless gene integration for pathway engineering in *Yarrowia lipolytica*. ACS Synth Biol 2017;6(3):402–9. https://doi.org/10.1021/acssynbio.6b00285.
[27] Fraser PD, Shimada H, Misawa N. Enzymic confirmation of reactions involved in routes to astaxanthin formation, elucidated using a direct substrate in vitro assay. Eur J Biochem 1998;252(2):229–36. https://doi.org/10.1046/j.1432-1327.1998.2520229.x.
[28] Liu J, Sun Z, Gerken H, Liu Z, Jiang Y, Chen F. *Chlorella zofingiensis* as an alternative microalgal producer of astaxanthin: biology and industrial potential. Mar Drugs 2014;12(6):3487–515. https://doi.org/10.3390/md12063487.
[29] Roth MS, Cokus SJ, Gallaher SD, Walter A, Lopez D, Erickson E, et al. Chromosome-level genome assembly and transcriptome of the green alga *Chromochloris zofingiensis* illuminates astaxanthin production. Proc Natl Acad Sci U S A 2017;114(21):E4296–305. https://doi.org/10.1073/pnas.1619928114.
[30] Ye Y, Huang JC. Defining the biosynthesis of ketocarotenoids in *Chromochloris zofingiensis*. Plant Divers 2020;42(1):61–6. https://doi.org/10.1016/j.pld.2019.11.001.
[31] Fraser PD, Miura Y, Misawa N. In vitro characterization of astaxanthin biosynthetic enzymes. J Biol Chem 1997;272(10):6128–35. https://doi.org/10.1074/jbc.272.10.6128.
[32] Lohr M, Im CS, Grossman AR. Genome-based examination of chlorophyll and carotenoid biosynthesis in *Chlamydomonas reinhardtii*. Plant Physiol 2005;138(1):490–515. https://doi.org/10.1104/pp.104.056069.
[33] Park SY, Binkley RM, Kim WJ, Lee MH, Lee SY. Metabolic engineering of *Escherichia coli* for high-level astaxanthin production with high productivity. Metab Eng 2018;49:105–15. https://doi.org/10.1016/j.ymben.2018.08.002.
[34] Lin YJ, Chang JJ, Lin HY, Thia C, Kao YY, Huang CC, et al. Metabolic engineering a yeast to produce astaxanthin. Bioresour Technol 2017;245(Pt A):899–905. https://doi.org/10.1016/j.biortech.2017.07.116.
[35] Chen SC, Chang LY, Wang YW, Chen YC, Weng KF, Shih SR, et al. Sumoylation-promoted enterovirus 71 3C degradation correlates with a reduction in viral replication and cell apoptosis. J Biol Chem 2011;286(36):31373–84. https://doi.org/10.1074/jbc.M111.254896.
[36] Schwartz C, Frogue K, Misa J, Wheeldon I. Host and pathway engineering for enhanced lycopene biosynthesis in *Yarrowia lipolytica*. Front Microbiol 2017;8:2233. https://doi.org/10.3389/fmicb.2017.02233.
[37] Vranova E, Coman D, Gruissem W. Network analysis of the MVA and MEP pathways for isoprenoid synthesis. Annu Rev Plant Biol 2013;64:665–700. https://doi.org/10.1146/annurev-arplant-050312-120116.
[38] Mora G, Scharnewski M, Fulda M. Neutral lipid metabolism influences phospholipid synthesis and deacylation in *Saccharomyces cerevisiae*. PLoS One 2012;7(11):e49269. https://doi.org/10.1371/journal.pone.0049269.
[39] Matthaus F, Ketelhot M, Gatter M, Barth G. Production of lycopene in the non-carotenoid-producing yeast *Yarrowia lipolytica*. Appl Environ Microbiol 2014;80(5):1660–9. https://doi.org/10.1128/AEM.03167-13.
[40] Larroude M, Celinska E, Back A, Thomas S, Nicaud JM, Ledesma-Amaro R. A synthetic biology approach to transform *Yarrowia lipolytica* into a competitive biotechnological producer of beta-carotene. Biotechnol Bioeng 2018;115(2):464–72. https://doi.org/10.1002/bit.26473.
[41] Gu Y, Jiao X, Ye L, Yu H. Metabolic engineering strategies for de novo biosynthesis of sterols and steroids in yeast. Bioresour Bioprocess 2021;8(1). https://doi.org/10.1186/s40643-021-00460-9.
[42] Gutierrez MS, Campusano S, Gonzalez AM, Gomez M, Barahona S, Sepulveda D, et al. Sterol regulatory element-binding protein (Sre1) promotes the synthesis of carotenoids and sterols in *Xanthophyllomyces dendrorhous*. Front Microbiol 2019;10:586. https://doi.org/10.3389/fmicb.2019.00586.
[43] Gomez M, Gutierrez MS, Gonzalez AM, Garate-Castro C, Sepulveda D, Barahona S, et al. Metallopeptidase Stp1 activates the transcription factor Sre1 in the carotenogenic yeast *Xanthophyllomyces dendrorhous*. J Lipid Res 2020;61(2):229–43. https://doi.org/10.1194/jlr.RA119000431.
[44] Gomez M, Campusano S, Gutierrez MS, Sepulveda D, Barahona S, Baeza M, et al. Sterol regulatory element-binding protein Sre1 regulates carotenogenesis in the red yeast *Xanthophyllomyces dendrorhous*. J Lipid Res 2020;61(12):1658–74. https://doi.org/10.1194/jlr.RA120000975.
[45] Qiao K, Wasylenko TM, Zhou K, Xu P, Stephanopoulos G. Lipid production in *Yarrowia lipolytica* is maximized by engineering cytosolic redox metabolism. Nat Biotechnol 2017;35(2):173–7. https://doi.org/10.1038/nbt.3763.
[46] Yu T, Zhou YJ, Huang M, Liu Q, Pereira R, David F, et al. Reprogramming yeast metabolism from alcoholic fermentation to lipogenesis. Cell 2018;174(6):1549–58. https://doi.org/10.1016/j.cell.2018.07.013. e14.
[47] Jin CC, Zhang JL, Song H, Cao YX. Boosting the biosynthesis of betulinic acid and related triterpenoids in *Yarrowia lipolytica* via multimodular metabolic engineering. Microb Cell Factories 2019;18(1):77. https://doi.org/10.1186/s12934-019-1127-8.
[48] Wasylenko TM, Ahn WS, Stephanopoulos G. The oxidative pentose phosphate pathway is the primary source of NADPH for lipid overproduction from glucose in *Yarrowia lipolytica*. Metab Eng 2015;30:27–39. https://doi.org/10.1016/j.ymben.2015.02.007.
[49] Goto S, Kogure K, Abe K, Kimata Y, Kitahama K, Yamashita E, et al. Efficient radical trapping at the surface and inside the phospholipid membrane is responsible for highly potent antiperoxidative activity of the carotenoid astaxanthin. Biochim Biophys Acta Biomembr 2001;1512(2, 6):251–8. https://doi.org/10.1016/S0005-2736(01)00326-1.
[50] Liu X, Liu M, Zhang J, Chang Y, Cui Z, Ji B, et al. Mapping of nonhomologous end joining-mediated integration facilitates genome-scale trackable mutagenesis in *Yarrowia lipolytica*. ACS Synth Biol 2022;11(1):216–27. https://doi.org/10.1021/acssynbio.1c00390.
[51] Lv PJ, Qiang S, Liu L, Hu CY, Meng YH. Dissolved-oxygen feedback control fermentation for enhancing β-carotene in engineered *Yarrowia lipolytica*. Sci Rep 2020;10(1):1–11. https://doi.org/10.1038/s41598-020-74074-0.